NASA
Technical
Paper
2830

November 1988

Eikonal Solutions to Optical Model Coupled-Channel Equations

Francis A. Cucinotta,
Govind S. Khandelwal,
Khin M. Maung,
Lawrence W. Townsend,
and John W. Wilson

NASA

NASA
Technical
Paper
2830

1988

Eikonal Solutions to Optical Model Coupled-Channel Equations

Francis A. Cucinotta,
Govind S. Khandelwal,
and Khin M. Maung
Old Dominion University
Norfolk, Virginia

Lawrence W. Townsend
and John W. Wilson
Langley Research Center
Hampton, Virginia

National Aeronautics
and Space Administration

**Scientific and Technical
Information Division**

Introduction

For career astronauts and long-duration missions, the high-energy heavy-ion component of galactic cosmic rays may cause harmful radiobiological effects. To assess these effects, an accurate theoretical description of the transport of high-energy nuclei through spacecraft structures is being developed (ref. 1). Essential inputs to this transport theory are reaction and fragmentation cross sections for heavy-ion collisions at cosmic ray energies.

In previous work, an optical model for composite particle scattering (refs. 2 through 7) had been solved to first order in the optical potential within the eikonal approximation to predict reaction and fragmentation cross sections but through indirect means. Here only the elastic channel in the coherent approximation, which neglects contributions of scattering to excited states with rescatterings to the ground state, is considered. The optical theorem allows for the calculation of the total cross section from the elastic amplitude, and the reaction cross section is then taken as the difference between the total and total elastic cross sections. Fragmentation cross sections are obtained by distributing the reaction cross section between the various fragmentation channels (ref. 6). This method gives good agreement with experimental measurements for reaction cross sections, although some discrepancies are seen for fragmentation cross sections which may be due to neglecting the contribution of bound-state inelastic transitions to the reaction cross section and/or misunderstanding ablation effects. One advantage of this approach is that the only nuclear structure inputs needed are ground state matter densities which are accurately determined from parameterization of experimentally measured nuclear charge densities.

The coherent approximation for the elastic channel and the distorted wave Born approximation (DWBA) for inelastic transitions represent lowest order solutions to coupled-channel equations derived in the optical model. In this work we consider methods for obtaining higher order solutions to the eikonal form of these coupled-channel equations. A nucleus will have an infinite number of levels for which nearly all excited state wave functions are poorly known but will represent necessary inputs for a complete solution to the coupled-channel equations. In the forward-scattering region, a limited number of low lying states may lead to a reasonable truncation of the infinite channel space for a light nucleus, although at high energies all nuclear levels will appear degenerate so that the accuracy of any channel truncation will depend on the strength and momentum dependence of the excited state wave functions. Alternatively, solutions exact through second or higher orders in the optical potential may be reexpressed using sum rules to incorporate pair or higher number correlation functions. Here the lack of knowledge of excited state wave functions is shifted to uncertainties in the correlation functions.

In the next section we review the eikonal formalism (refs. 2 and 3). Following this we discuss several approaches for obtaining solutions to the coupled-channel scattering amplitudes. Analytic forms are obtained for the second-order optical potential (bordered interaction matrix), which we apply to calculate angular distributions and total cross sections for elastic and inelastic scattering of p on ^{12}C and ^{4}He on ^{12}C. Comparisons are made between the first-order and second-order solutions.

Eikonal Coupled-Channels Formalism

In reference 2, a coupled-channel (Schröedinger) equation is obtained from a nonrelativistic multiple-scattering series for two composite particles through the use of an effective potential and the impulse and closure approximations. The coupled-channel equation relating the entrance channel to all excited states of the composite target and projectile particles is

$$\left(\nabla_{\mathbf{x}}^2 + \mathbf{k}^2\right) \psi_{n\mu}(\mathbf{x}) = \frac{2mA_PA_T}{A_P + A_T} \sum_{n'\mu'} V_{n\mu,n'\mu'}(\mathbf{x})\, \psi_{n'\mu'}(\mathbf{x}) \tag{1}$$

where the subscripts n and μ label the eigenstates of projectile and target, respectively; $\mathbf{k}$ is the projectile momentum relative to the center of mass; $\psi_{n\mu}$ is the channel wave function; $\mathbf{x}$ is the projectile position vector relative to the target; A_P and A_T are the projectile and target constituent numbers; and m is the constituent mass. The coupling potentials are of the form

$$V_{n\mu,n'\mu'}(\mathbf{x}) = \langle g_n g_\mu | V_{\text{opt}} | g_{n'} g_{\mu'} \rangle \tag{2}$$

where g represents the internal nuclear wave function, and the effective potential is given by

$$V_{\text{opt}} = \sum_{\alpha j}^{A_P, A_T} t_{\alpha j} \tag{3}$$

where $t_{\alpha j}$ is the two-body transition amplitude. Equation (1) represents the complete solution to the nucleus-nucleus scattering system within the high-energy approximations noted.

Matrix notation is introduced by defining the wave vector,

$$\overline{\Psi}(\mathbf{x}) = \begin{bmatrix} \psi_{00}(\mathbf{x}) \\ \psi_{01}(\mathbf{x}) \\ \psi_{10}(\mathbf{x}) \\ \psi_{11}(\mathbf{x}) \\ \cdot \\ \cdot \\ \cdot \end{bmatrix} \tag{4}$$

and the potential matrix

$$\overline{\mathbf{U}}(\mathbf{x}) = \mu_R \begin{bmatrix} V_{00,00}(\mathbf{x}) & V_{00,01}(\mathbf{x}) & V_{00,10}(\mathbf{x}) & \cdot & \cdot & \cdot \\ V_{01,00}(\mathbf{x}) & V_{01,01}(\mathbf{x}) & V_{01,10}(\mathbf{x}) & \cdot & \cdot & \cdot \\ V_{10,00}(\mathbf{x}) & V_{10,01}(\mathbf{x}) & V_{10,10}(\mathbf{x}) & \cdot & \cdot & \cdot \\ V_{11,00}(\mathbf{x}) & V_{11,01}(\mathbf{x}) & V_{11,10}(\mathbf{x}) & \cdot & \cdot & \cdot \\ \cdot & \cdot & \cdot & & & \\ \cdot & \cdot & \cdot & & & \\ \cdot & \cdot & \cdot & & & \end{bmatrix} \tag{5}$$

where we have denoted the reduced mass factor by μ_R and have arranged the elements of $\overline{\Psi}(\mathbf{x})$ and $\overline{\mathbf{U}}(\mathbf{x})$ in order of increasing levels of target, followed by projectile excitation. The coupled equations are then written in matrix form

$$\left(\nabla_{\mathbf{x}}^2 + \mathbf{k}^2\right) \overline{\Psi}(\mathbf{x}) = \overline{\mathbf{U}}(\mathbf{x})\, \overline{\Psi}(\mathbf{x}) \tag{6}$$

The scattering amplitudes for all transitions, n, μ to n', μ', are the elements of the scattering amplitude matrix which is written

$$\bar{\mathbf{f}}(\mathbf{q}) = -\sqrt{\frac{\pi}{2}} \int e^{-i\mathbf{k}_f \cdot \mathbf{x}}\, \overline{\mathbf{U}}(\mathbf{x})\, \overline{\Psi}(\mathbf{x})\, d\mathbf{x} \tag{7}$$

where $\mathbf{k}_f$ is the final projectile momentum and $\mathbf{q}$ the momentum transfer,

$$\mathbf{q} = \mathbf{k} - \mathbf{k}_f \tag{8}$$

In references 2 and 3, the eikonal approximation was applied to the coupled-channel formalism. Here we outline the derivation of $\bar{\mathbf{f}}(\mathbf{q})$ in the eikonal approximation. In this forward-scattering approximation, the following boundary condition is imposed on the wave vector:

$$\lim_{z \to -\infty} \overline{\Psi}(\mathbf{x}) = \left(\frac{1}{2\pi}\right)^{3/2} e^{i\mathbf{k}\cdot\mathbf{x}} \bar{\delta} \tag{9}$$

where $-z$ is the direction of the beam source and $\overline{\delta}$ is a constant vector with a unit entry at the entrance channel and zero elsewhere. This boundary condition implies that no particles are scattered backward which is justified in high-energy scattering where forward scattering dominates. The wave vector is assumed to be of the form

$$\overline{\Psi}(\mathbf{x}) = \left(\frac{1}{2\pi}\right)^{3/2} \exp\left[i\,\overline{\Phi}(\mathbf{x})\right]\, e^{i\mathbf{k}\cdot\mathbf{x}}\overline{\delta} \tag{10}$$

where $\overline{\Phi}(\mathbf{x})$ is a phase matrix whose solution we seek. The boundary condition (eq. (9)) implies

$$\lim_{z \to -\infty} \overline{\Phi}(\mathbf{x}) = 0 \tag{11}$$

Substituting equation (10) into equation (6) with the approximations,

$$|\overline{\mathbf{U}}(\mathbf{x})| << \left|\mathbf{k}^2\right| \tag{12}$$

and

$$|\nabla_{\mathbf{x}}\,\overline{\mathbf{U}}(\mathbf{x})| << |\mathbf{k}\,\overline{\mathbf{U}}(\mathbf{x})| \tag{13}$$

leads to the solution

$$\overline{\Phi}(\mathbf{x}) = \frac{-1}{2k}\int_{-\infty}^{z} \overline{\mathbf{U}}(\mathbf{b}, z')\,dz' \tag{14}$$

where we use a cylindrical coordinate system with cylinder axis along the beam direction such that

$$\mathbf{x} = \mathbf{b} + \mathbf{z} \tag{15}$$

where $\mathbf{b}$ is the impact parameter vector. Finally, we ignore the longitudinal momentum transfer such that

$$\mathbf{q}\cdot\mathbf{x} = \mathbf{q}\cdot\mathbf{b} + 0(\theta^2) \tag{16}$$

where θ is the scattering angle, which is assumed to be small. The result for the scattering amplitude matrix in the eikonal approximation follows as

$$\overline{\mathbf{f}}(\mathbf{q}) = \frac{-ik}{2\pi}\int e^{-i\mathbf{q}\cdot\mathbf{b}}\left\{e^{i\overline{\chi}(\mathbf{b})} - \mathbf{1}\right\} d^2b \tag{17}$$

where the eikonal phase matrix is defined by

$$\overline{\chi}(\mathbf{b}) = \frac{-1}{2k}\int_{-\infty}^{\infty} \overline{\mathbf{U}}(\mathbf{b}, z)\,dz \tag{18}$$

and d^2b indicates integration over polar coordinates in the plane perpendicular to the incident direction of the beam.

We note that Feshbach and Hüfner (ref. 8) have considered the eikonal approximation for coupled-channel equations for nucleon-nucleus scattering. Here the *ansatz* of equation (10) is replaced by one equivalent to

$$\overline{\Psi}(\mathbf{x}) = \left(\frac{1}{2\pi}\right)^{3/2} \overline{\xi}(\mathbf{x})\, e^{i\mathbf{k}\cdot\mathbf{x}}\overline{\delta} \tag{19}$$

Feshbach and Hüfner found that a solution such as equation (17) can be obtained only if the commutator

$$\left[\overline{\mathbf{U}}(\mathbf{b}, z), \int_{-\infty}^{z} dz'\ \overline{\mathbf{U}}(\mathbf{b}, z')\right] = 0 \tag{20}$$

is fulfilled. Through consideration of the form of the matrix elements of $\overline{\mathbf{U}}(\mathbf{x})$ in the momentum representation (see appendix A), we expect the condition given by equation (20) to be met in the limit when the longitudinal momentum transfer approaches zero.

Approximate solutions to the eikonal scattering amplitudes were discussed in reference 3. The exact solutions of these amplitudes have been hindered in the past by the mathematical difficulties inherent in identifying the elements of $\bar{\mathbf{f}}(\mathbf{q})$ with the corresponding elements of $\overline{\chi}(\mathbf{b})$ because of the occurrence of the exponential of the matrix $i\overline{\chi}(\mathbf{b})$. To appreciate this difficulty, consider two matrices $\overline{\mathbf{G}}$ and $\overline{\mathbf{B}}$ related by

$$\overline{\mathbf{G}} = e^{\overline{\mathbf{B}}}$$

We may make an expansion such that

$$\overline{\mathbf{G}} = \bar{\mathbf{1}} + \overline{\mathbf{B}} = \frac{\overline{\mathbf{B}}^2}{2!} + \frac{\overline{\mathbf{B}}^3}{3!} + \ldots$$

and the difficulty in obtaining the elements of $\overline{\mathbf{G}}$ in terms of the elements of $\overline{\mathbf{B}}$ is now obvious because we must construct all the powers of $\overline{\mathbf{B}}$ and then sum an infinite series for each element of $\overline{\mathbf{G}}$. In a similar manner the expansion of $\exp(i\overline{\chi})$ reveals the infinite-order multiple scattering series, including excitation and deexcitation of projectile and target in the eikonal limit. The exponential of the phase matrix has effectively summed this infinite series. In the next section, we consider possible methods for identifying the elements of the eikonal scattering amplitude matrix.

Methods of Solution for Eikonal Scattering Amplitudes

In this section we compare several approaches for identifying the elements of the scattering amplitude matrix as given in equation (17). The Cayley-Hamilton theorem states that every square matrix satisfies its own characteristic equation. The characteristic equation for the eikonal phase matrix is given by the determinant equation

$$|\overline{\chi} - \lambda\bar{\mathbf{1}}| = 0 \tag{21}$$

where λ represents the eigenvalues of $\overline{\chi}$. For $\overline{\chi}$ of rank N, equation (21) represents an Nth order polynomial in λ which must also hold for $\overline{\chi}$. Through this polynomial equation in $\overline{\chi}$, higher order powers of $\overline{\chi}$ can be expressed in terms of lower order powers which could allow for the summation of the infinite-order expansion of $\exp(i\overline{\chi})$. We do not expect the Cayley-Hamilton theorem to lead to a straightforward numerical procedure for summation of this series for an arbitrary form for $\overline{\chi}$.

A second approach for summation of this infinite series is through a similarity transformation. That is, if the unitary matrix $\overline{\mathbf{A}}$ diagonalizes $\overline{\chi}$ such that (ref. 9)

$$\overline{\mathbf{A}}^{\dagger}\overline{\chi}\overline{\mathbf{A}} = \overline{\mathbf{D}}(\lambda_\ell) \tag{22}$$

where $\overline{\mathbf{D}}$ is a diagonal matrix with the eigenvalues λ_ℓ of $\overline{\chi}$ along its diagonal, then

$$\exp(i\overline{\chi}) = \overline{\mathbf{A}}\,\overline{\mathbf{D}}\left(e^{i\lambda_\ell}\right)\overline{\mathbf{A}}^{\dagger} \tag{23}$$

and we find

$$\bar{\mathbf{f}}(\mathbf{q}) = \frac{-ik}{2\pi}\int e^{-i\mathbf{q}\cdot\mathbf{b}}\left\{\overline{\mathbf{A}}(\mathbf{b})\,\overline{\mathbf{D}}\left(e^{i\lambda_\ell(\mathbf{b})}\right)\overline{\mathbf{A}}^{\dagger}(\mathbf{b}) - \bar{\mathbf{1}}\right\} d^2b \tag{24}$$

The solution for the elements of $\bar{\mathbf{f}}(\mathbf{q})$ is now dependent on knowledge of the eigenvalues and eigenvectors of $\overline{\chi}$.

The elements of $\overline{\chi}$ are, in general, complex. A condition for a complex matrix to be similar to a diagonal matrix is that its real and imaginary parts be diagonalizable simultaneously, that is, that it be normal. This is equivalent to the commutation relation (ref. 10),

$$[\overline{\chi}, \overline{\chi}^{\dagger}] = 0 \tag{25}$$

In terms of real-space transition densities, the elements of $\overline{\chi}$ may be written (ref. 2) as

$$\chi_{n\mu,n'\mu'}(\mathbf{b}) = \frac{-\mu_R A_P A_T}{2k} \int_{-\infty}^{\infty} dz \int d\mathbf{x}' \, \rho_{\mu\mu'}(\mathbf{x}') \int d\mathbf{y} \, \rho_{nn'}(\mathbf{x}+\mathbf{x}'+\mathbf{y}) \, t(e,\mathbf{y}) \tag{26}$$

In appendix A we show that for transitions between states of discrete values of angular momentum the elements of $\overline{\chi}$ may be expressed in terms of reduced transition form factors, which are real, as

$$\begin{aligned} \chi_{J_P M_P, J_T M_T}(\mathbf{b}) = {} & \frac{-\mu_R A_P A_T}{2k} B_{J_P M_P} B_{J_T M_T} (-1)^{M_P + M_T} \\ & \times G_{J_P M_P, J_T M_T}(\mathbf{b}) \exp\left[-i(M_P + M_T)(\phi_b + \pi/2)\right] \end{aligned} \tag{27}$$

where $J_P = J_n - J_{n'}$, $J_T = J_\mu - J_{\mu'}$, $M_P = M_n - M_{n'}$, and $M_T = M_\mu - M_{\mu'}$. Because of the complex phase in equation (27), the condition for diagonalization as given by equation (25) will not be fulfilled for general values of M_P and M_T.

Finally, we consider use of Sylvester's theorem for identifying the elements of $\overline{\mathbf{f}}(\mathbf{q})$. Sylvester's theorem is based on the recognition that any polynomial relation that holds for a scalar variable will also be true for any square matrix. In particular (ref. 11), if we consider Lagrange's interpolation formula to hold for a polynomial P of the square matrix $\overline{\mathbf{B}}$, where $\overline{\mathbf{B}}$ has N distinct eigenvalues, choosing the interpolation coefficients to be the eigenvalues, Sylvester's theorem states

$$P(\overline{\mathbf{B}}) = \sum_{\ell=1}^{N} P(\lambda_\ell) \prod_{\substack{j=1 \\ j\neq\ell}}^{N} \frac{(\lambda_j \overline{\mathbf{1}} - \overline{\mathbf{B}})}{(\lambda_j - \lambda_\ell)} \tag{28}$$

The extension of Sylvester's theorem to the infinite series represented by $\exp(i\overline{\chi})$ depends on convergence conditions required for the exponential of a matrix (ref. 11) which we assume to be true. Then

$$\exp(i\overline{\chi}) = \sum_{\ell=1}^{N} e^{i\lambda_\ell} \prod_{\substack{j=1 \\ j\neq\ell}}^{N} \frac{(\lambda_j \overline{\mathbf{1}} - \overline{\chi})}{(\lambda_j - \lambda_\ell)} \tag{29}$$

The extension to the case of degenerate roots is considered in reference 11. Here if s is the degeneracy of the root, then

$$\exp(i\overline{\chi}) = \sum \frac{1}{s-1} \left\{ \frac{d^{s-1}}{d\lambda^{s-1}} \left[\frac{e^{i\lambda} \operatorname{adj} \overline{\chi}}{\Delta_s(\lambda)} \right] \right\}_{\lambda=\lambda_s} \tag{30}$$

where

$$\Delta_s(\lambda) = (\lambda - \lambda_{s+1})(\lambda - \lambda_{s+2}) \ldots (\lambda - \lambda_N) \tag{31}$$

The solution that follows from application of Sylvester's theorem offers the advantage that only the eigenvalues and not the eigenvectors of $\overline{\chi}$ are needed and should lead to a straightforward numerical procedure for identifying the elements of $\overline{\mathbf{f}}(\mathbf{q})$. From equation (30) we expect that this method will not be practical if a large degeneracy occurs. In the next section, we consider a bordered form for $\overline{\chi}$ where analytic methods allow us to solve for the form of the scattering amplitudes with any of the three methods discussed.

Bordered Interaction Matrix

The bordered interaction matrix neglects couplings between all excited states, which for the elastic channel leads to a solution that is exact through second order in the optical potential (ref. 8). In this

section we consider solutions to equation (17) for a bordered interaction matrix of the form

$$\bar{\chi} = \begin{vmatrix} \chi_{opt} & \chi_{00,01} & \chi_{00,01} & \chi_{00,11} & \cdot & \cdot & \cdot \\ \chi_{01,00} & \chi_{opt} & 0 & 0 & \cdot & \cdot & \cdot \\ \chi_{10,00} & 0 & \chi_{opt} & 0 & \cdot & \cdot & \cdot \\ \chi_{11,00} & 0 & 0 & \chi_{opt} & \cdot & \cdot & \cdot \\ \cdot & \cdot & \cdot & \cdot & & & \\ \cdot & \cdot & \cdot & \cdot & & & \\ \cdot & \cdot & \cdot & \cdot & & & \end{vmatrix} \tag{32}$$

where

$$\chi_{opt} = \chi_{00,00} \tag{33}$$

Here the density of the excited nuclear medium is taken to be approximately the same as the ground state. The validity of this approximation should increase with mass number and has been estimated to introduce an error of approximately 15 percent for ^{4}He and 2.5 percent for ^{16}O (ref. 8).

In appendix B we find the characteristic equation for a matrix of rank N of the bordered form, from which we arrive at the following equation:

$$(\chi_{opt} - \lambda)^2 = \sum_{(n,\mu)\neq(0,0)} \chi_{00,n\mu}\,\chi_{n\mu,00} \tag{34}$$

A direct application of the Cayley-Hamilton theorem allows us to obtain analytic expressions for all scattering amplitudes. Define

$$\Upsilon^2 = \sum_{n,\mu\neq(0,0)} \chi_{00,n\mu}\,\chi_{n\mu,00} \tag{35}$$

and from equation (34) we find

$$\lambda^2 = 2\chi_{opt}\lambda + \Upsilon^2 - \chi_{opt}^2 \tag{36}$$

All higher powers of λ may be found in terms of expressions linear in λ. For example,

$$\lambda^3 = \left[3\chi_{opt}^2 + \Upsilon^2\right]\lambda + 2\chi_{opt}\Upsilon^2 - 2\chi_{opt}^3 \tag{37}$$

$$\lambda^4 = \left[4\chi_{opt}^3 + 4\chi_{opt}\Upsilon^2\right]\lambda - 3\chi_{opt}^4 + \Upsilon^4 + 2\chi_{opt}^2\Upsilon^2 \tag{38}$$

and

$$\lambda^5 = \left[5\chi_{opt}^4 + 10\chi_{opt}^2\Upsilon^2 + \Upsilon^4\right]\lambda + 4\chi_{opt}\Upsilon^4 - 4\chi_{opt}^5 \tag{39}$$

By the Cayley-Hamilton theorem, equation (34) must also hold when λ is replaced by $\bar{\chi}$. Consider

$$\exp(i\bar{\chi}) = \bar{1} + i\bar{\chi} - \frac{1}{2!}\bar{\chi}^2 - \frac{i}{3!}\bar{\chi}^3 + \frac{1}{4!}\bar{\chi}^4 + \frac{i}{5!}\bar{\chi}^5 + \ldots \tag{40}$$

Substituting from equations (32) and (36) through (39) into equation (40) gives

$$\begin{aligned}[\exp(i\bar{\chi})]_{00,00} = 1 + i\chi_{opt} - \frac{1}{2!}(\chi_{opt}^2 + \Upsilon^2) - \frac{i}{3!}(\chi_{opt}^3 + 3\chi_{opt}\Upsilon^2) \\ + \frac{1}{4!}(\chi_{opt}^4 + \Upsilon^4 + 6\chi_{opt}^2\Upsilon^2) + \frac{i}{5!}(\chi_{opt}^5 + 5\chi_{opt}\Upsilon^4 + 14\chi_{opt}^3\Upsilon^2)\end{aligned} \tag{41}$$

Rearranging terms gives

$$[\exp(i\overline{\chi})]_{00,00} = \left(1 + i\chi_{\text{opt}} - \frac{1}{2!}\chi_{\text{opt}}^2 - \frac{i}{3!}\chi_{\text{opt}}^3 + \ldots\right)\left(1 - \frac{\Upsilon^2}{2!} + \frac{\Upsilon^4}{4!} + \ldots\right) \tag{42}$$

which we recognize as

$$[\exp(i\overline{\chi})]_{00,00} = e^{i\chi_{\text{opt}}} \cos \Upsilon \tag{43}$$

Similarly

$$\begin{aligned}[\exp(i\overline{\chi})]_{00,n\mu} = i\chi_{00,n\mu}\Big\{1 + i\chi_{\text{opt}} - \frac{1}{2!}\chi_{\text{opt}}^2 - \frac{1}{3!}\Upsilon^2 - \frac{i}{3!}\chi_{\text{opt}}^3 - \frac{i}{3!}\chi_{\text{opt}}\Upsilon^2 \\ + \frac{1}{4!}\chi_{\text{opt}}^4 + \frac{2}{4!}\chi_{\text{opt}}^2\Upsilon^2 + \frac{1}{5!}\Upsilon^4 + \ldots\Big\}\end{aligned} \tag{44}$$

and rearranging terms gives

$$[\exp(i\overline{\chi})]_{00,n\mu} = i\chi_{00,n\mu}\left\{\left(1 + i\chi_{\text{opt}} - \frac{1}{2!}\chi_{\text{opt}}^2 - \frac{i}{3!}\chi_{\text{opt}}^3 + \ldots\right)\left(1 - \frac{\Upsilon^2}{3!} + \frac{\Upsilon^4}{5!} + \ldots\right)\right\} \tag{45}$$

which we recognize as

$$[\exp(\overline{\chi})]_{00,n\mu} = i\chi_{00,n\mu}\, e^{i\chi_{\text{opt}}} \frac{\sin \Upsilon}{\Upsilon} \tag{46}$$

From equation (17), we now identify the scattering amplitudes as

$$f_{\text{elas}}(\mathbf{q}) = \frac{-ik}{2\pi} \int e^{-i\mathbf{q}\cdot\mathbf{b}} \left\{e^{i\chi_{\text{opt}}} \cos \Upsilon - 1\right\} d^2b \tag{47}$$

and

$$f_{00,n\mu}(\mathbf{q}) = \frac{k}{2\pi} \int e^{-i\mathbf{q}\cdot\mathbf{b}} e^{i\chi_{\text{opt}}} \frac{\sin \Upsilon}{\Upsilon} \chi_{00,n\mu}\, d^2b \tag{48}$$

In reference 8 analogous results have been obtained by using the method of similarity transformation. We note that although $\overline{\chi}$ is not normal, this method is applicable because not all eigenvectors are needed to obtain equations (47) and (48). From the form of the characteristic equation (see appendix B),

$$(\chi_{\text{opt}} - \lambda)^{N-2}\left[(\chi_{\text{opt}} - \lambda)^2 - \Upsilon^2\right] = 0 \tag{49}$$

We recognize the eigenvalues of $\overline{\chi}$ as

$$\left.\begin{aligned}\lambda_1 &= \chi_{\text{opt}} + \Upsilon \\ \lambda_2 &= \chi_{\text{opt}} \\ &\cdot \\ &\cdot \\ &\cdot \\ \lambda_{N-1} &= \chi_{\text{opt}} \\ \lambda_N &= \chi_{\text{opt}} - \Upsilon\end{aligned}\right\} \tag{50}$$

It is then straightforward to obtain equations (43) and (46) with Sylvester's theorem but tedious to generalize to arbitrary rank N.

We note that the coherent and DWBA approximations are recovered from equations (47) and (48), respectively, in the limit of small Υ. Also, in general, the function Υ will have a dependence on the

azimuthal angle ϕ_b (fig. 1), such that a numerical integration over this angle will be required for the second-order solutions.

The function Υ as given in equation (35) is directly related to the pair correlation function. This can be seen by substitution of equation (A9) into equation (35),

$$\Upsilon^2 = \left(\frac{\mu_r}{2k}\right)^2 \left(\frac{1}{2\pi}\right)^4 \int d^2q\, d^2q'\, e^{-i\mathbf{q}\cdot\mathbf{b}}\, e^{-i\mathbf{q}'\cdot\mathbf{b}} \times \sum_{\mu \text{ or } n\neq 0}^{\infty} F_{0n}(\mathbf{q})\, F_{n0}(\mathbf{q}')\, F_{0\mu}(-\mathbf{q})\, F_{\mu 0}(-\mathbf{q}') \times t(\mathbf{q})\, t(\mathbf{q}') \tag{51}$$

From reference 12, we have the following sum rule on the form factors

$$\sum_{n\neq 0}^{\infty} F_{0n}(\mathbf{q})\, F_{n0}(\mathbf{q}) = \frac{-1}{A} F_{00}(\mathbf{q})\, F_{00}(\mathbf{q}') + \frac{1}{A} F_{00}(\mathbf{q}+\mathbf{q}') + \left(1 - \frac{1}{A}\right) C_{00}(\mathbf{q},\mathbf{q}) \tag{52}$$

where A is the mass number of the nucleus in question and $C_{00}(\mathbf{q},\mathbf{q}')$ is the Fourier transform of the pair correlation function. Analytic models for $C_{00}(\mathbf{q},\mathbf{q}')$ are under investigation. In the next section we consider a numerical study of long-range correlations involving partial summation of the infinite summation that appears in equation (51) for ^{12}C.

Finally, we note that the first- and second-order solutions to the eikonal coupled-channel scattering amplitudes were found by approximating the form of $\overline{\chi}$. We expect that higher order solutions, though more difficult, could be found by approximating the form of higher powers of $\overline{\chi}$.

Physical Inputs

As a numerical study, we compare the first- and second-order eikonal coupled-channel solutions for p on ^{12}C and ^{4}He on ^{12}C scattering. The 2^+ at 4.65 MeV, 0^+ at 7.66 MeV, 3^- at 9.65 MeV, and 4^+ at 14.1 MeV excited states of ^{12}C are considered. An advantage of the bordered interaction matrix is that the eikonal phase matrix elements may be obtained through knowledge of form factors measured in electron scattering experiments, so that no excited state wave functions are needed as inputs. This would not be true for couplings between the off-diagonal elements. The charge form factors for the ground and first three excited states have been parameterized previously (refs. 13 and 14) in the form

$$F_{\text{charge}}(q) = B\, q^m (1 - Cq^2)\, e^{-dq^2} \tag{53}$$

where the parameters B, C, d, and m are listed in table I. Table I also lists the form factor for excitation of the 4^+ state at 14.1 MeV of ^{12}C which we have parameterized to the data of reference 15.

The matter form factors are obtained from the charge form factors in the following manner (ref. 16)

$$F_A(q) = \frac{F_{\text{charge}}(q)}{F_p(q)\, F_{cm}(q)} \tag{54}$$

where $F_p(q)$ is the proton charge form factor given by

$$F_p(q) = e^{-r_p q^2/6} \tag{55}$$

with $r_p = 0.87$ fm, and $F_{cm}(q)$ is a center-of-mass correction of the form

$$F_{cm}(q) = e^{+q^2 a_0^2/4A} \tag{56}$$

with

$$a_0^2 = \frac{< r^2 > - r_p^2}{\frac{z-2}{z} + \frac{3(A-1)}{2A}} \tag{57}$$

where $< r^2 >$ is the root-mean-square radius of the nucleus. For the ground state of ^{4}He, we use the parameterization of reference 17,

$$F_{^4\mathrm{He}} = C_1\, e^{-d_1 q^2} - C_2\, e^{-d_2 q^2} \tag{58}$$

where C_1, C_2, d_1, and d_2 are listed in table I.

The two-body amplitude is assumed to contain only a central piece of the usual form (ref. 2)

$$t(q) = -\sqrt{\frac{e}{m}}\sigma(e)[\alpha(e) + i]\, e^{-\frac{1}{2}B(e)q^2} \tag{59}$$

where the energy-dependent parameters $\sigma(e), \alpha(e)$ and $B(e)$ are taken from reference 18 and given in table II.

The Gaussian forms for the form factors and two-body amplitude assumed in our calculation allow us to obtain analytic solutions for all eikonal phase matrix elements needed as inputs for our calculations. All integrals needed are of the form listed in appendix C.

Results and Discussion

The first- and second-order scattering solutions and experimental data for elastic and inelastic scattering of p on ^{12}C at 800 MeV (ref. 19) and 1000 MeV (ref. 20) and for ^{4}He on ^{12}C at 340A MeV (ref. 21) are shown in figures 2 through 12. For p–^{12}C elastic scattering (figs. 2 and 6), the coherent approximation (dashed line) and bordered matrix (solid line) results are nearly identical in the region of the forward peak where single scattering dominates. We include Coulomb effects only in an approximate way assuming a point Coulomb interaction. A more exact treatment is needed to completely fill in the first minimum. (See, for example, refs. 21 and 22.) Here spin effects may also be important (refs. 17 and 23). The effect of coupling the elastic channel to low-lying excited states is seen in the second maximum (figs. 2 and 6) where the bordered matrix agrees well, whereas the coherent approximation underestimates the data both at 800 and 1000 MeV. The sensitivity to the number of channels included in the second-order calculations can be seen in figure 7 where the dashed line includes only the 2^+ state; the long-dash–short-dash line, the 2^+ and 0^+ states; and the solid line, the 2^+, 0^+, 3^-, and 4^+ states. At larger angles, agreement with the data is poor. Here the validity of the eikonal approximation is suspect, and the momentum transfers being probed are beyond the region where the phenomenological fits to the form factors and two-body amplitudes are made. For the second-order solutions, the effects of channel truncation, including the neglect of short-range correlations, in the Υ-function may be more important at larger angles.

Calculations of the excitation of the 2^+, 0^+, and 3^- excited states of ^{12}C by 800 and 1000 MeV protons are shown in figures 3 through 5 and 8 through 10, respectively. The dashed line is the DWBA and the solid line is the bordered matrix (second-order) solution. The formalism for the DWBA is given in appendix D. For all excited states, the DWBA and bordered matrix give similar results in the region of the first and second maxima. We note that although the bordered matrix contains all couplings to second order for the elastic channel, the cascades between excited, which are neglected, should be considered a second-order effect for inelastic transitions. These cascades would be most important in the region of the second maximum. In the region of the third maximum, we do see better agreement for the bordered matrix solutions as compared with the DWBA for all transitions considered.

In figures 11 and 12 we show calculations, respectively, for elastic scattering and excitation of the 0^+ state of ^{12}C for 340A MeV ^{4}He on ^{12}C collisions. The experimental results of reference 21 do not report the forward peak with the data beginning at approximately 5°. We do not include any correlation effects for ^{4}He in our calculations. The importance of correlations is expected to increase for the lightest nuclei (ref. 24).

In table III we list total cross sections for all channels considered for p–^{12}C scattering at 340, 800, and 1000 MeV. The total of the cross sections is calculated by the optical theorem, and the reaction

cross section is taken as the difference between the total and total elastic cross sections. The first- and second-order results are nearly the same for all channels. This agreement is expected because our angular distributions show almost complete agreement between the two solutions in the forward angles where most of the cross section occurs. In table III we also sum the cross sections for the bound-excited (BE) states calculated, $\sigma(\mathrm{BE})$. We note that $\sigma(\mathrm{BE})$ represents only a small fraction, <5 percent, of the total reaction cross section, which is an indication that the neglect of the bound excited states in the abrasion model (ref. 6) is a good approximation, although the importance of the giant dipole resonance state should be estimated.

Concluding Remarks

We have presented several approaches for solving the eikonal form of the coupled-channel scattering amplitudes. Analytic forms for second-order solutions have been obtained, and their relationship to the pair correlation function established. Improved agreement with experimental results for p–$^{12}\mathrm{C}$ scattering is seen for the second-order solutions in comparison with the coherent approximation and the distorted wave Born approximation. Second-order effects are seen to make a negligible contribution to total channel cross sections. Future work should involve inclusion of spin effects and the development of analytic models for the pair correlation function.

NASA Langley Research Center
Hampton, VA 23665-5225
September 1, 1988

Appendix A

Eikonal Phase Matrix Elements in Terms of Momentum Space Representations

In this appendix, we reexpress the real space eikonal phase matrix elements in terms of the momentum space representations of the transition densities and two-body amplitude. This allows us to explicitly show the complex dependence of these matrix elements.

If projectile and target total angular momentum transfer numbers are defined as

$$\left.\begin{aligned} J_P &= J_n - J_{n'} \\ J_T &= J_\mu - J_{\mu'} \end{aligned}\right\} \tag{A1}$$

and total projection angular momentum transfer numbers are defined as

$$\left.\begin{aligned} M_P &= M_n - M_{n'} \\ M_T &= M_\mu - M_{\mu'} \end{aligned}\right\} \tag{A2}$$

we introduce the projectile and target transition form factors $F_{J_P M_P}$ and $F_{J_T M_T}$, respectively, given by

$$\rho_{J_P M_P}(\mathbf{x}+\mathbf{y}+\boldsymbol{\xi}) = \frac{1}{(2\pi)^3}\int d\mathbf{q}\, e^{-i(\mathbf{x}+\mathbf{y}+\boldsymbol{\xi})\cdot\mathbf{q}}\, F_{J_P M_P}(\mathbf{q}) \tag{A3}$$

and

$$\rho_{J_T M_T}(\boldsymbol{\xi}) = \frac{1}{(2\pi)^3}\int d\mathbf{q}\, e^{-i\boldsymbol{\xi}\cdot\mathbf{q}'}\, F_{J_T M_T}(\mathbf{q}') \tag{A4}$$

and the momentum-space representation of the two-body amplitude given by

$$t(\mathbf{y}) = \frac{1}{(2\pi)^3}\int d\mathbf{q}''\, e^{-i\mathbf{y}\cdot\mathbf{q}''}\, t(\mathbf{q}'') \tag{A5}$$

into equation (26) to find

$$\chi_{J_P M_P, J_T M_T}(\mathbf{b}) = \frac{-\mu r}{2k}\frac{1}{(2\pi)^3}\int_{-\infty}^{\infty} dz \int d\mathbf{q}\, e^{-i\mathbf{q}\cdot\mathbf{x}} F_{J_P M_P}(-\mathbf{q})\, F_{J_T M_T}(\mathbf{q})\, t(\mathbf{q}) \tag{A6}$$

In the eikonal approximation, the parallel momentum transfer is assumed to be negligible. Letting

$$\mathbf{q}\cdot\mathbf{x} = \mathbf{q}_\perp\cdot\mathbf{b} + q_\parallel z \tag{A7}$$

such that $\mathbf{q}_\perp$ and $\mathbf{b}$ lie in the x-y plane (fig. 1) and assuming the $q_\parallel$ dependence of the form factors and two-body amplitude approaches zero faster than $\exp(-iq_\parallel z)$ gives

$$\chi_{J_P M_P, J_T M_T} = \frac{-\mu r}{2k}\frac{1}{(2\pi)^3}\int_{-\infty}^{\infty} dz \int_0^{\infty} dq_\parallel\, e^{-iq_\parallel z}\int d\mathbf{q} e^{-i\mathbf{q}_\perp\cdot\mathbf{b}} F_{J_P M_P}(-\mathbf{q})\, F_{J_T M_T}(+\mathbf{q})\, t(\mathbf{q}) \tag{A8}$$

which reduces to

$$\chi_{J_P M_P, J_T M_T}(\mathbf{b}) = \frac{-\mu r}{2k}\frac{1}{(2\pi)^2}\int d^2q\, e^{-i\mathbf{q}\cdot\mathbf{b}}\, F_{J_P M_P}(-\mathbf{q})\, F_{J_T M_T}(\mathbf{q})\, t(\mathbf{q}) \tag{A9}$$

where $\mathbf{q}_\perp$ has been replaced by $\mathbf{q}$. Next, we introduce reduced form factors $F_J(q)$ defined by

$$F_{JM}(\mathbf{q}) = \sqrt{\frac{4\pi}{2J+1}}\, Y^*_{JM}(\theta_q, \phi_q)\; F_J(q) \tag{A10}$$

where

$$Y_{JM}(\theta_q, \phi_q) = (-1)^M \sqrt{\frac{2J+1}{4\pi}} \sqrt{\frac{(J-M)!}{(J+M)!}} P_{JM}(\cos\theta_q)\, e^{-iM\phi_q} \tag{A11}$$

and where P_{JM} represents the associated Legendre polynomials. From figure 1 we can see that $\theta_q = \frac{\pi}{2}$, and using the identity (ref. 25),

$$P_{JM}\left(\theta_q = \frac{\pi}{2}\right) = \left\{ \begin{array}{cc} 0 & (J+M = \text{odd}) \\ \dfrac{(-1)^{(J-M)/2}(J+M-1)!!}{(J-M)!!} & (J+M = \text{even}) \end{array} \right\} \tag{A12}$$

then defining coupling coefficients as

$$B_{JM} = \sqrt{\frac{(J-M)!}{(J+M)!}}\, \frac{(J+M-1)!!}{(J-M)!!} \tag{A13}$$

gives

$$Y^*_{JM}\left(\frac{\pi}{2}, \phi_q\right) = \sqrt{\frac{2J+1}{4\pi}} B_{JM}\, e^{-iM\phi_q} \tag{A14}$$

Substituting equations (A10) and (A14) into equation (A9) yields

$$\chi_{J_P M_P, J_T M_T}(\mathbf{b}) = \frac{-\mu r}{2k} \frac{1}{(2\pi)^2} B_{J_P M_P}\, B_{J_T M_T} \int d^2q\, e^{-i\mathbf{q}\cdot\mathbf{b}}\, e^{-i(M_P+M_T)\phi_q}\, F_{J_P}(-q)\, F_{J_T}(q)\, t(\mathbf{q}) \tag{A15}$$

Then using

$$\mathbf{q}\cdot\mathbf{b} = qb\cos(\phi_b - \phi_q) \tag{A16}$$

and using the identities (ref. 25)

$$\int_0^{2\pi} e^{n\phi_1}\, e^{-ixy\cos(\phi_1-\phi_2)}\, d\phi_2 = 2\pi(-i)^n\, e^{in\phi_1}\, J_n(xy) \tag{A17}$$

and

$$J_{-n} = (-1)^n J_n \tag{A18}$$

where J_n, the Bessel function of order n, gives the final result as follows:

$$\chi_{J_P M_P, J_T M_T}(\mathbf{b}) = \frac{-\mu r}{4\pi} B_{J_P M_P}\, B_{J_T M_T} (-1)^{(M_P+M_T)} G_{J_P M_P, J_T M_T}(\mathbf{b})\, e^{-i(M_P+M_T)(\phi_b+\pi/2)} \tag{A19}$$

where we have defined

$$G_{J_P M_P, J_T M_T}(\mathbf{b}) = \int_0^\infty q\, dq\, J_{(M_P+M_T)}(qb)\, F_{J_P}(q)\, F_{J_T}(q)\, t(q) \tag{A20}$$

The complex dependence of the eikonal phase matrix elements is now explicitly shown in equation (A19) to occur in the exponential phase and in any complex dependence in $t(q)$. We note, also, that equation (A19) offers considerable computational advantage over equation (26).

Appendix B
Characteristic Equation for Bordered Matrix

In this appendix, we prove that a bordered matrix of the form

$$\overline{\mathbf{B}}_N = \begin{bmatrix} b_{1,1} & b_{1,2} & b_{1,3} & \cdot & \cdot & \cdot & b_{1,N} \\ b_{2,1} & d & 0 & \cdot & \cdot & \cdot & 0 \\ b_{3,1} & 0 & d & \cdot & \cdot & \cdot & 0 \\ \cdot & \cdot & \cdot & \cdot & \cdot & \cdot & \cdot \\ \cdot & \cdot & \cdot & \cdot & \cdot & \cdot & \cdot \\ \cdot & \cdot & \cdot & \cdot & \cdot & \cdot & \cdot \\ b_{N,1} & 0 & 0 & \cdot & \cdot & \cdot & d \end{bmatrix} \tag{B1}$$

of rank N has a characteristic equation of the form

$$(d-\lambda)^{N-2}\left[(b_{1,1}-\lambda)(d-\lambda) - \sum_{\ell=2}^{N} b_{1,\ell}b_{\ell,1}\right] = 0 \tag{B2}$$

where the eigenvalues of $\overline{\mathbf{B}}_N$ are λ.

Proof: To prove that equation (B2) holds, we consider the cofactor expansion of the characteristic determinant of $\overline{\mathbf{B}}_N$ and use induction with respect to rank. The result is easily seen to be true by inspection for small N so our proof is complete.

The characteristic determinant of $\overline{\mathbf{B}}_N$ is written

$$|\overline{\mathbf{D}}_N| = |\overline{\mathbf{B}}_N - \lambda\overline{\mathbf{I}}| = 0 \tag{B3}$$

A determinant can be expanded in terms of the cofactor matrices of any of its rows or columns. Choosing the first row of $\overline{\mathbf{D}}_N$ to make the cofactor expansion gives

$$|\overline{\mathbf{D}}_N| = \sum_{\ell=1}^{N} d_{1,\ell}\,\overline{\mathbf{A}}_{1,\ell} \tag{B4}$$

or

$$|\overline{\mathbf{D}}_N| = \sum_{\ell=1}^{N} d_{1,\ell}(-1)^{1+\ell}\,|\overline{\mathbf{D}}_{1,\ell}| \tag{B5}$$

where $\overline{\mathbf{A}}_{1,\ell}$ is the cofactor corresponding to the element $d_{1,\ell}$, and $|\overline{\mathbf{D}}_{1,\ell}|$ is the related determinant. If equation (B1) is used, we find

$$|\overline{\mathbf{D}}_N| = (b_{1,1}-\lambda)(-1)^{1+1}|\overline{\mathbf{D}}_{1,1}| + b_{1,2}(-1)^{1+2}|\overline{\mathbf{D}}_{1,2}| + \ldots + b_{1,N}(-1)^{1+N}|\overline{\mathbf{D}}_{1,N}| \tag{B6}$$

By assumption we must have

$$|\overline{\mathbf{D}}_N| = (b_{1,1}-\lambda)(d-\lambda)^{N-1} - b_{1,2}b_{2,1}(d-\lambda)^{N-2} - \ldots - b_{1,N}b_{N,1}(d-\lambda)^{N-2} = 0 \tag{B7}$$

such that

$$\left.\begin{aligned} |\overline{\mathbf{D}}_{1,1}| &= (d-\lambda)^{N-1} \\ |\overline{\mathbf{D}}_{1,2}| &= -(-1)^{1+2}b_{2,1}(d-\lambda)^{N-2} \\ &\cdot \\ &\cdot \\ &\cdot \\ |\overline{\mathbf{D}}_{1,N}| &= -(-1)^{1+N}b_{1,N}(d-\lambda)^{N-2} \end{aligned}\right\} \tag{B8}$$

in order for equation (B2) to be correct.

Consider a bordered matrix of the form given by equation (B1) of rank $N+1$. We have

$$|\overline{\mathbf{D}}'_{N+1}| = (b_{1,1}-\lambda)|\overline{\mathbf{D}}'_{1,1}| + (-1)^{1+2}b_{1,2}|\overline{\mathbf{D}}'_{1,2}| + \ldots + b_{1,N+1}(-1)^{1+(N+1)}|\overline{\mathbf{D}}'_{1,N+1}| \tag{B9}$$

On comparison of equations (B7) and (B9), we see that to complete the proof we must show

$$\left.\begin{aligned} |\overline{\mathbf{D}}'_{1,1}| &= (d-\lambda)^N \\ &\vdots \\ |\overline{\mathbf{D}}'_{1,2}| &= (d-\lambda)|\overline{\mathbf{D}}_{1,2}| \\ &\vdots \\ |\overline{\mathbf{D}}'_{1,3}| &= (d-\lambda)|\overline{\mathbf{D}}_{1,3}| \\ &\vdots \\ |\overline{\mathbf{D}}'_{1,N}| &= (d-\lambda)|\overline{\mathbf{D}}_{1,N}| \\ &\vdots \\ |\overline{\mathbf{D}}'_{1,N+1}| &= -(d-\lambda)^{N-1}b_{1,N+1} \end{aligned}\right\} \tag{B10}$$

That

$$|\overline{\mathbf{D}}'_{1,1}| = (d-\lambda)^N \tag{B11}$$

is easily seen by inspection. Consider

$$|\overline{\mathbf{D}}_{1,2}| = \begin{vmatrix} b_{2,1} & 0 & 0 & \cdots & 0 \\ b_{3,1} & d-\lambda & 0 & \cdots & 0 \\ b_{4,1} & 0 & d-\lambda & \cdots & 0 \\ \cdot & \cdot & \cdot & \cdots & \cdot \\ \cdot & \cdot & \cdot & \cdots & \cdot \\ \cdot & \cdot & \cdot & \cdots & \cdot \\ b_{1,N} & 0 & 0 & \cdots & d-\lambda \end{vmatrix} \tag{B12}$$

and

$$|\overline{\mathbf{D}}'_{1,2}| = \begin{vmatrix} b_{2,1} & d-\lambda & 0 & \cdots & 0 & 0 \\ b_{3,1} & 0 & d-\lambda & \cdots & 0 & 0 \\ b_{4,1} & 0 & 0 & \cdots & 0 & 0 \\ \cdot & \cdot & \cdot & \cdots & \cdot & \cdot \\ \cdot & \cdot & \cdot & \cdots & \cdot & \cdot \\ \cdot & \cdot & \cdot & \cdots & \cdot & \cdot \\ b_{N,1} & 0 & 0 & \cdots & d-\lambda & 0 \\ b_{N+1,1} & 0 & 0 & \cdots & 0 & d-\lambda \end{vmatrix} \tag{B13}$$

For $|\overline{\mathbf{D}}'_{1,2}|$, we make a cofactor expansion about the last column to find

$$|\overline{\mathbf{D}}'_{1,2}| = (-1)^{N+N}|\overline{\mathbf{D}}'_{1,2}|(d-\lambda) \tag{B14}$$

therefore,

$$|\overline{\mathbf{D}}'_{1,2}| = (d = \lambda)|\overline{\mathbf{D}}_{1,2}| \tag{B15}$$

A similar result that holds for $|\overline{\mathbf{D}}'_{1,3}|$ through $|\overline{\mathbf{D}}'_{1,N}|$ is easily seen by inspection. Finally, consider $|\overline{\mathbf{D}}'_{1,N+1}|$

$$|\overline{\mathbf{D}}'_{1,N+1}| = \begin{vmatrix} b_{2,1} & d-\lambda & 0 & \cdot & \cdot & \cdot & 0 & 0 \\ b_{3,1} & 0 & d-\lambda & \cdot & \cdot & \cdot & 0 & 0 \\ b_{4,1} & 0 & 0 & \cdot & \cdot & \cdot & 0 & 0 \\ \cdot & \cdot & \cdot & \cdot & \cdot & \cdot & \cdot & \cdot \\ \cdot & \cdot & \cdot & \cdot & \cdot & \cdot & \cdot & \cdot \\ \cdot & \cdot & \cdot & \cdot & \cdot & \cdot & \cdot & \cdot \\ b_{N,1} & 0 & 0 & \cdot & \cdot & \cdot & 0 & (d-\lambda) \\ b_{N+1,1} & 0 & 0 & \cdot & \cdot & \cdot & 0 & 0 \end{vmatrix} \tag{B16}$$

Making the cofactor expansion about the last row gives

$$|\overline{\mathbf{D}}_{1,N+1}| = -(d-\lambda)^{N-1} b_{N+1,1} \tag{B17}$$

Thus our proof is complete.

Appendix C

Analytic Forms for G_{JM} Integrals

In this appendix, we tabulate analytic forms for the functions $G_{JM}(qb)$ as defined in equation (A20) when Gaussians are used for form factors and the two-body amplitude. All integrals tabulated may be generated from the integral (ref. 26),

$$\int_0^\infty q^{\mu+1}\, e^{-aq^2} J_\mu(qb)\, dq = \frac{b^\mu}{(2a)^{\mu+1}}\, e^{-b^2/4a} \tag{C1}$$

where μ is a positive integer by differentiation with respect to the parameter a. Defining

$$J_\alpha^\beta = \int_0^\infty q^\beta\, e^{-aq^2} J_\alpha(qb)\, dq \tag{C2}$$

these integrals are given as follows:

$$J_0^1 = \frac{1}{2a}\, e^{-b^2/4a} \tag{C3}$$

$$J_0^3 = \frac{1}{2a^2}\left(1 - \frac{b^2}{4a}\right) e^{-b^2/4a} \tag{C4}$$

$$J_0^5 = \frac{1}{a^3}\left(1 - \frac{b^2}{2a} + \frac{b^4}{32a^3}\right) e^{-b^2/4a} \tag{C5}$$

$$J_1^2 = \frac{b}{4a^2}\, e^{-b^2/4a} \tag{C6}$$

$$J_1^4 = \frac{b}{2a^3}\left(1 - \frac{b^2}{4a}\right) e^{-b^2/4a} \tag{C7}$$

$$J_1^6 = \frac{b}{2a^4}\left(3 - \frac{5b^2}{4a} + \frac{b^4}{32a^2}\right) e^{-b^2/4a} \tag{C8}$$

$$J_2^3 = \frac{b^2}{8a^3}\, e^{-b^2/4a} \tag{C9}$$

$$J_2^5 = \frac{b^2}{8a^4}\left(3 - \frac{b^2}{4a}\right) e^{-b^2/4a} \tag{C10}$$

$$J_3^4 = \frac{b^3}{16a^4}\, e^{-b^2/4a} \tag{C11}$$

$$J_3^6 = \frac{b^3}{4a^5}\left(1 - \frac{b^2}{16a}\right) e^{-b^2/4a} \tag{C12}$$

$$J_4^5 = \frac{b^4}{32a^5}\, e^{-b^2/4a} \tag{C13}$$

Appendix D
Distorted Wave Born Approximation

In this appendix, we obtain the form of the distorted wave Born approximation (DWBA) that follows from use of equation (A18) for the eikonal phase matrix elements. From references 2 and 3, the DWBA for the scattering amplitude has the following form in the eikonal approximated, optical model formalism:

$$f_{J_P M_P, J_T M_T}(\mathbf{q}) = \frac{k}{2\pi} \int e^{-i\mathbf{q}\cdot\mathbf{b}}\, e^{i\chi_{\rm opt}(\mathbf{b})}\, \chi_{J_P M_P, J_T M_T}(\mathbf{b})\, d^2b \tag{D1}$$

where $\chi_{\rm opt}(\mathbf{b})$ is the elastic element $\chi_{00,00}(\mathbf{b})$. Substitution of equation (A19) into equation (D1) gives

$$\begin{aligned} f_{J_P M_P, J_T M_T}(\mathbf{q}) = {} & \frac{-\mu r}{8\pi^2} B_{J_P M_P}\, B_{J_T M_T} (-1)^{(M_P + M_T)} (-i)^{(M_P + M_T)} \\ & \times \int e^{-i\mathbf{q}\cdot\mathbf{b}} e^{i(M_P + M_T)\phi_b} e^{i\chi_{\rm opt}(\mathbf{b})} G_{J_P M_P, J_T M_T}(\mathbf{b}) \end{aligned} \tag{D2}$$

Then with

$$\mathbf{q}\cdot\mathbf{b} = qb\cos(\phi_b - \phi_q) \tag{D3}$$

and the identities (A17) and (A18), we find

$$\begin{aligned} f_{J_P M_P, J_T M_T}(\mathbf{q}) = {} & \frac{-\mu r}{4\pi} B_{J_P M_P}\, B_{J_T M_T} \\ & \times \int_0^\infty b\, db\, J_{(M_P + M_T)}(qb) e^{i\chi_{\rm opt}(\mathbf{b})} G_{J_P M_P, J_T M_T}(\mathbf{b}) \end{aligned} \tag{D4}$$

where we have dropped an inconsequential phase. The form of the angular distribution for a discrete projectile-target transition then follows as

$$\begin{aligned} \frac{d\sigma}{d\Omega}(J_P M_P, J_T M_T) = {} & \left|\frac{\mathbf{P}_F}{\mathbf{P}_i}\right| \sum_{M_{n'}, M_{\mu'}} \left|\frac{\mu r}{4\pi} B_{J_P M_P} B_{J_T M_T}\right. \\ & \left. \times \int_0^\infty b\, db\, J_{(M_P + M_T)}(qb)\; e^{i\chi_{\rm opt}(b)}\, G_{J_P M_P, J_T M_T}(\mathbf{b})\right|^2 \end{aligned} \tag{D5}$$

where $\mathbf{P}_i$ and $\mathbf{P}_F$ are the initial and final center-of-mass momenta of the projectile, respectively. Values for the coupling coefficients, for small values of J, are listed in table IV.

References

1. Wilson, J. W.; Townsend, L. W.; and Badavi, F. F.: Galactic HZE Propagation Through the Earth's Atmosphere. *Radiat. Res.*, vol. 109, no. 2, Feb. 1987, pp. 173–183.
2. Wilson, John W.: Composite Particle Reaction Theory. Ph.D. Diss., College of William and Mary in Virginia, June 1975.
3. Wilson, John W.; and Costner, Christopher M.: *Nucleon and Heavy-Ion Total and Absorption Cross Section for Selected Nuclei.* NASA TN D-8107, 1975.
4. Wilson, J. W.; and Townsend, L. W.: An Optical Model for Composite Nuclear Scattering. *Canadian J. Phys.*, vol. 59, no. 11, Nov. 1981, pp. 1569–1576.
5. Townsend, Lawrence W.; Wilson, John W.; and Bidasaria, Hari B.: *Heavy-Ion Total and Absorption Cross Sections Above 25 MeV/Nucleon.* NASA TP-2138, 1983.
6. Townsend, Lawrence W.: *Optical-Model Abrasion Cross Sections for High-Energy Heavy Ions.* NASA TP-1893, 1981.
7. Townsend, L. W.; Wilson, J. W.; Cucinotta, F. A.; and Norbury, J. W.: Comparison of Abrasion Model Differences in Heavy Ion Fragmentation: Optical Versus Geometric Models. *Phys. Review C,* vol. 34, third ser., no. 4, Oct. 1986, pp. 1491–1494.
8. Feshbach, H.; and Hüfner, J.: On Scattering by Nuclei at High Energies. *Ann. Phys.*, vol. 56, no. 1, Jan. 1970, pp. 268–294.
9. Mirsky, L.: *An Introduction to Linear Algebra.* Clarendon Press (Oxford), 1955.
10. Mathews, Jon; and Walker, R. L.: *Mathematical Methods of Physics,* Second ed. W. A. Benjamin, Inc., c.1970.
11. Frazer, R. A.; Duncan, W. J.; and Collar, A. R.: *Elementary Matrices and Some Applications to Dynamics and Differential Equations.* Cambridge: At the University Press, 1947.
12. Kerman, A. K.; McManus, H.; and Thaler, R. M.: The Scattering of Fast Nucleons From Nuclei. *Ann. Phys. (N.Y.),* vol. 8, no. 4, Dec. 1959, pp. 551–635.
13. Saudinos, Jean; and Wilkin, Colin: Proton-Nucleus Scattering at Medium Energies. *Annual Review of Nuclear Science,* Volume 24, Emilio Segrè, J. Robb Grover, and H. Pierre Noyes, eds., Annual Reviews Inc., 1974, pp. 341–377.
14. Viollier, R. D.: High-Energy Proton-Nucleus Scattering and Correlations. *Ann. Phys.*, vol. 93, no. 1-2, Sept. 5, 1975, pp. 335–368.
15. Nakada, A.; Torizuka, Y.; and Horikawa, Y.: Determination of the Deformation in ^{12}C From Electron Scattering. *Phys. Review Lett.*, vol. 27, no. 11, Sept. 13, 1971, pp. 745–748.
16. Überall, Herbert: *Electron Scattering From Complex Nuclei, Part A.* Academic Press, Inc., 1971.
17. Auger, J. P.; Gillespie, J.; and Lombard, R. J.: Proton-^{4}He Elastic Scattering at Intermediate Energies. *Nucl. Phys.*, vol. A262, no. 3, May 24, 1976, pp. 372–388.
18. Ray, L.: Proton-Nucleus Total Cross Sections in the Intermediate Energy Range. *Phys. Review C,* vol. 20, third ser., no. 5, Nov. 1979, pp. 1857–1872.
19. Blanpied, G. S.; Hoffman, G. W.; et al.: Large Angle Scattering of 0.8 GeV Protons From ^{12}C. *Phys. Review C,* vol. 23, third ser., no. 6, June 1981, pp. 2599–2605.
20. Bertini, R.; Buertey, R.; et al.: Angular Distribution of 1.04 GeV Protons Scattered by ^{12}C, ^{58}Ni, ^{208}Pb. *Phys. Lett.*, vol. 45B, no. 2, July 9, 1973, pp. 119–122.
21. Chaumeaux, A.; Bruge, G.; et al.: Scattering of 1.37 GeV α-Particles by ^{12}C. *Nucl. Phys.*, vol. A267, no. 3, Aug. 30, 1976, pp. 413–424.
22. Glauber, R. J.; and Matthiae, G.: High-Energy Scattering of Protons by Nuclei. *Nucl. Phys.*, vol. B21, no. 1, Aug. 1, 1970, pp. 135–157.
23. Ahmad, I.: An Analysis of Some Proton-Nucleus Scattering Data at 1 GeV. *Nucl. Phys.*, vol. A247, no. 3, Aug. 11, 1975, pp. 418–440.
24. Feshbach, Herman; Gal, Avraham; and Hüfner, Jörg: On High-Energy Scattering by Nuclei—II. *Ann. Phys.*, vol. 66, no. 1, July 1971, pp. 20–59.
25. Arfken, George: *Mathematical Methods for Physicists.* Academic Press, Inc., c.1966.
26. Gradshteyn, I. S.; and Ryzhik, I. M. (Scripta Technica, Inc., transl.): *Table of Integrals, Series, and Products,* Corrected & Enlarged ed. Academic Press, Inc., 1980.

Table I. Form Factors

(a) ^{12}C

E, MeV	J^P	m	B	C	d, fm^{-2}
0	0^+	0	1.0	0.296	0.7
4.43	2^+	2	0.24	0.13	0.57
7.65	0^+	2	0.167	0	0.99
9.67	3^-	3	0.134	0	0.77
14.1	4^+	4	0.00392	0	0.64

(b) ^4He

$C_1 = 1.098$
$C_2 = 0.098$
$d_1 = 0.72$
$d_2 = 3.6$

Table II. Two-Body Amplitude Parameters

[Isospin averaged parameters of reference 18]

T_{lab}, MeV	$B(e)$, fm^2	$\sigma(e)$, fm^2	$\alpha(e)$
340	0.62	3.03	0.28
800	0.20	4.3	–0.056
1000	0.21	4.3	–0.26

Table III. Total Channel Cross Sections for p on ^{12}C

Cross section	T_{lab} = 340 MeV		T_{lab} = 800 MeV		T_{lab} = 1000 MeV	
	Coherent	Bordered	Coherent	Bordered	Coherent	Bordered
σ(EL), mb	54.1	53.5	92.5	91.3	103.5	102.1
σ(BE), mb	3.5	3.5	7.1	7.1	7.5	7.5
$\sigma(2^+)$, mb	2.2	2.2	4.1	4.1	4.3	4.3
$\sigma(0^+)$, mb	0.3	0.3	0.4	0.4	0.4	0.4
$\sigma(3^-)$, mb	1.0	1.0	2.5	2.5	2.6	2.6
$\sigma(4^+)$, mb	0.03	0.03	0.1	0.1	0.1	0.1
σ(re), mb	220.9	220.3	238.3	237.2	223.8	223.0
σ(tot), mb	275.0	273.8	330.8	328.5	327.3	325.1

Table IV. Values for Coupled Coefficients

J	M	B_{JM}*
0	0	1
1	1	$1/\sqrt{2}$
2	0	$1/2$
2	2	$\sqrt{6/4}$
3	1	$\sqrt{3/4}$
3	3	$\sqrt{5/4}$
4	0	$3/8$
4	2	$\sqrt{5/32}$
4	4	$\sqrt{35/128}$

*$B_{J-M} = B_{JM}$

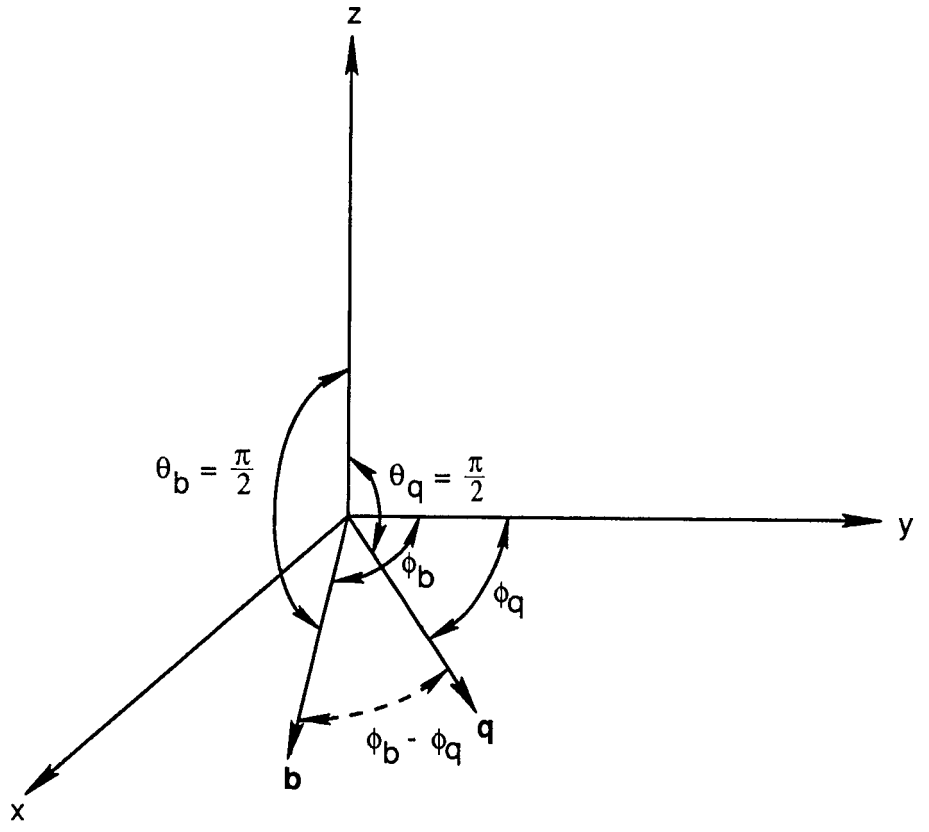

Figure 1. Orientation of momentum vector and impact parameter vector in scattering plane.

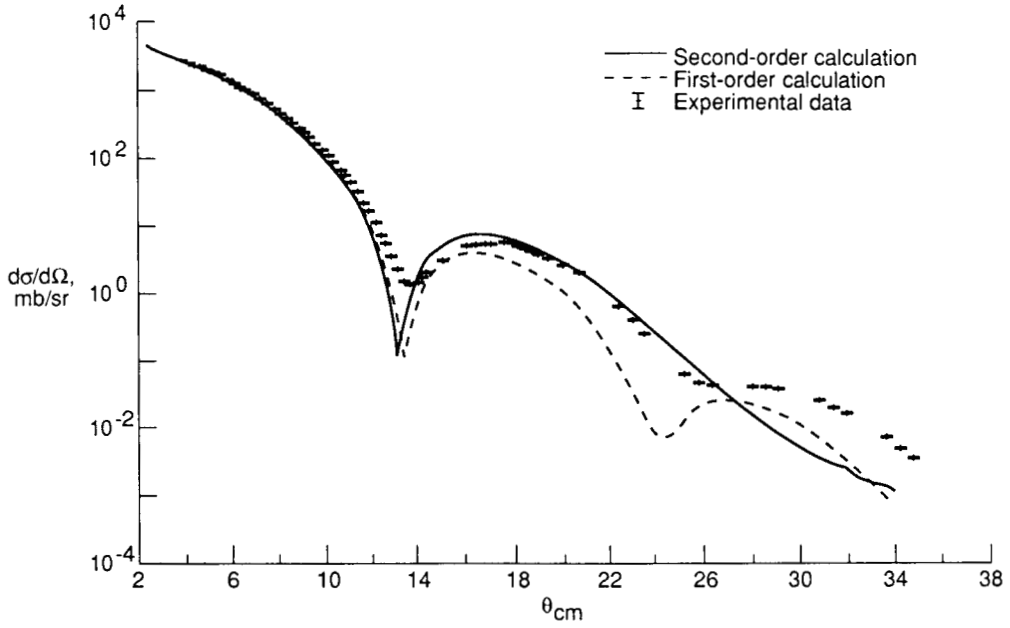

Figure 2. Theoretical and experimental (ref. 19) elastic angular distributions for 800 MeV p–^{12}C scattering.

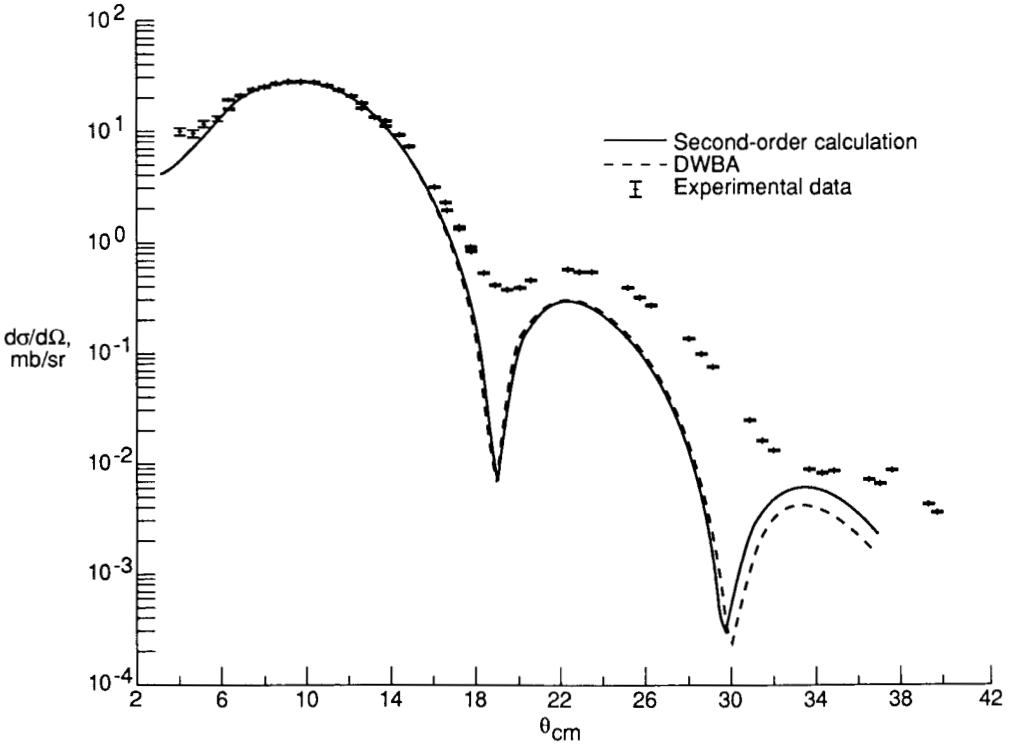

Figure 3. Theoretical and experimental (ref. 19) inelastic angular distributions for excitation of 2^+ state in ^{12}C in 800 MeV p–^{12}C scattering.

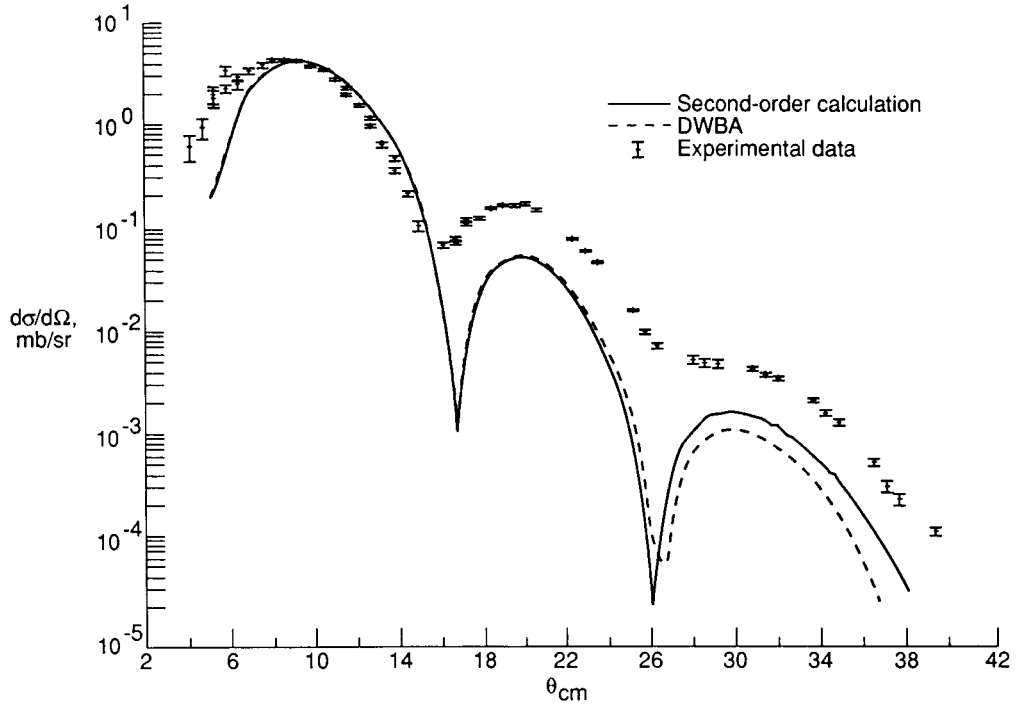

Figure 4. Theoretical and experimental (ref. 19) inelastic angular distributions for excitation of 0^+ state of ^{12}C.

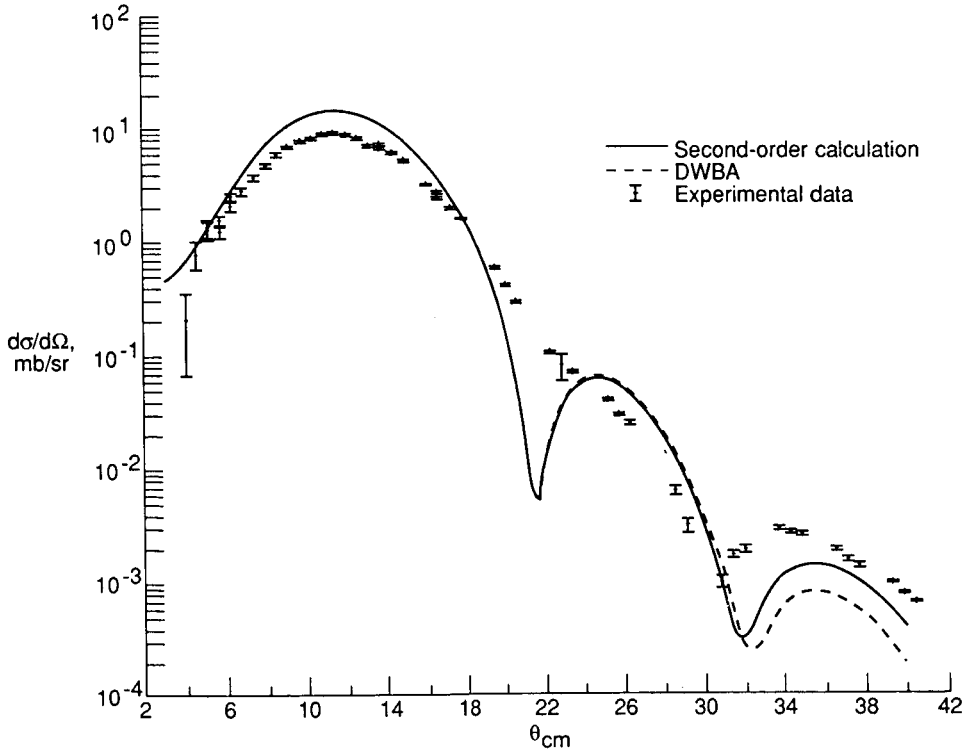

Figure 5. Theoretical and experimental (ref. 19) inelastic angular distributions for excitation of 3^- state of ^{12}C.

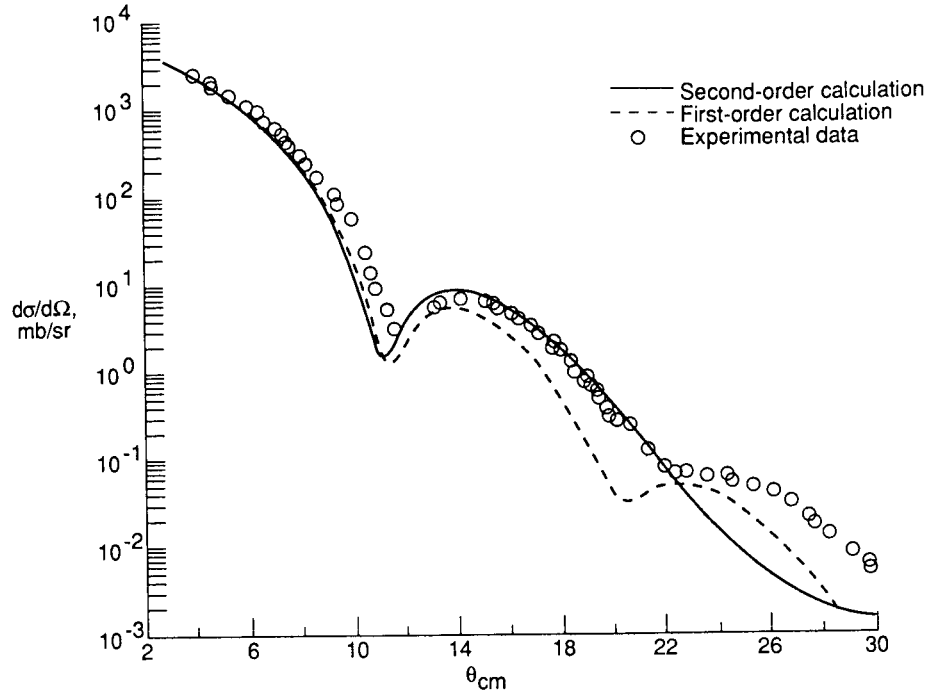

Figure 6. Theoretical and experimental (ref. 20) elastic angular distributions for 1040 MeV p–^{12}C scattering.

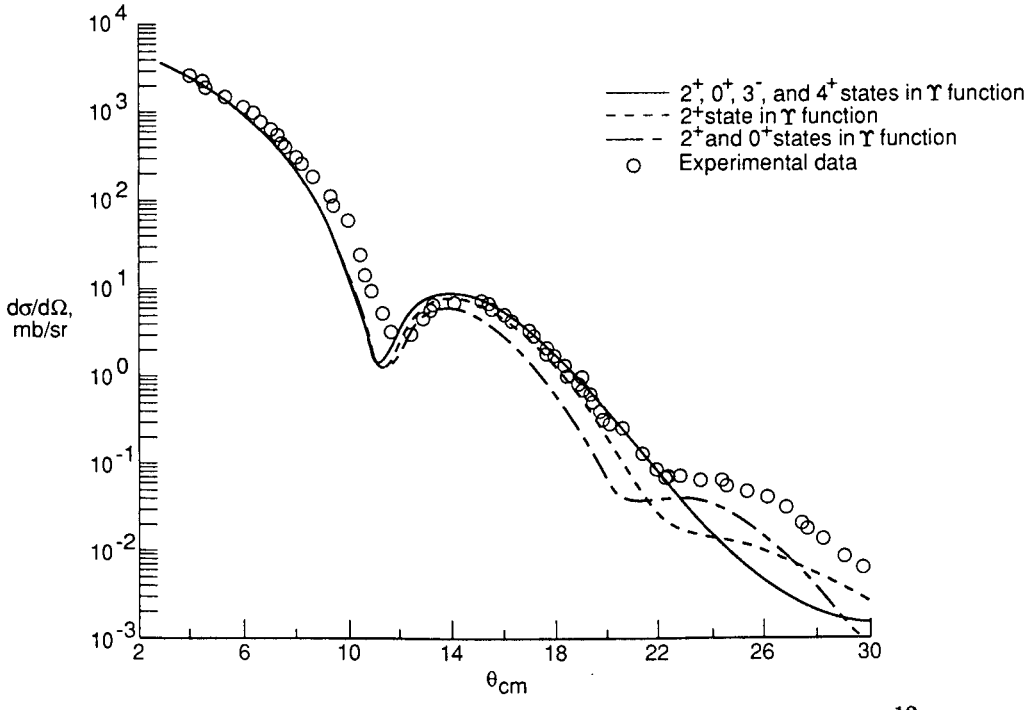

Figure 7. Effect of channel truncation in second-order calculations for 1040 MeV p–^{12}C elastic scattering.

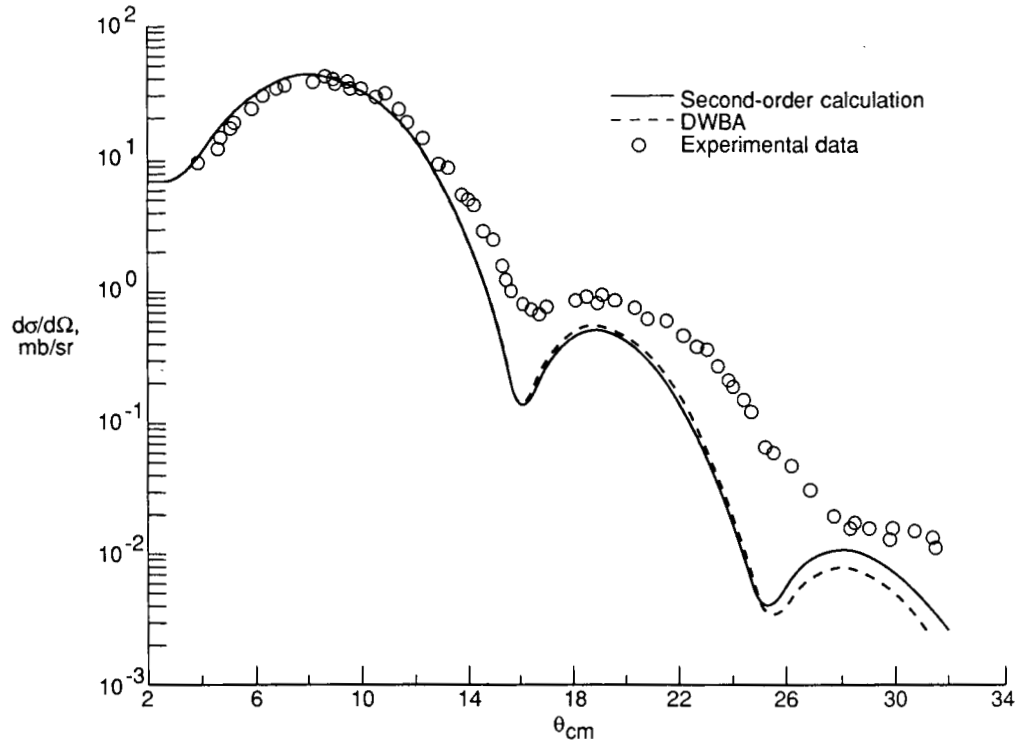

Figure 8. Theoretical and experimental (ref. 20) inelastic angular distributions for excitation of 2^+ state in ^{12}C in 1040 MeV p–^{12}C scattering.

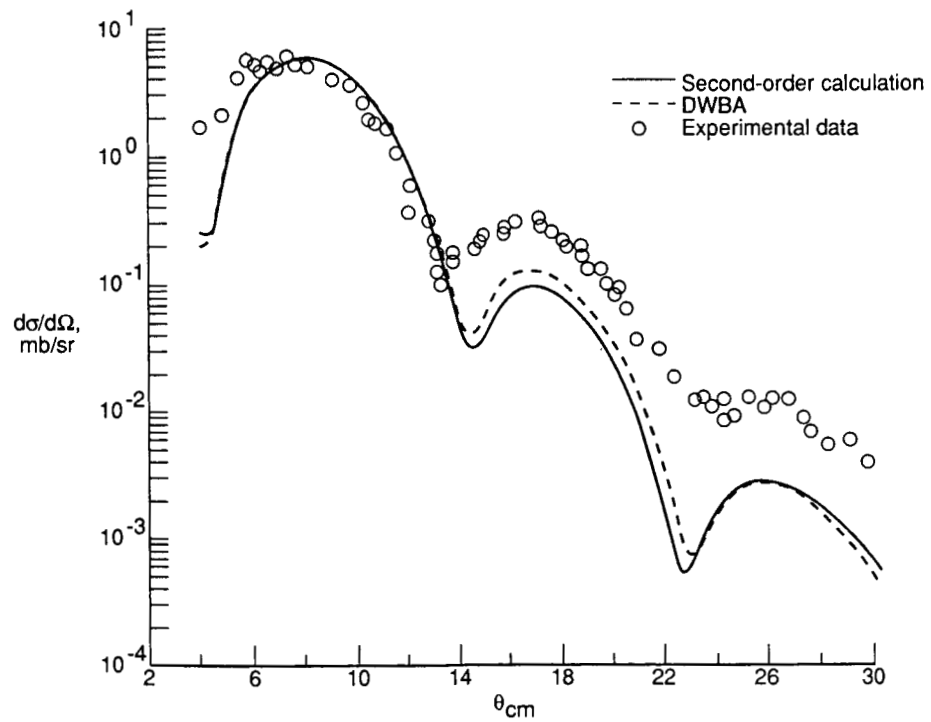

Figure 9. Theoretical and experimental (ref. 20) inelastic angular distributions for excitation of 0^+ state in ^{12}C in 1040 MeV p–^{12}C scattering.

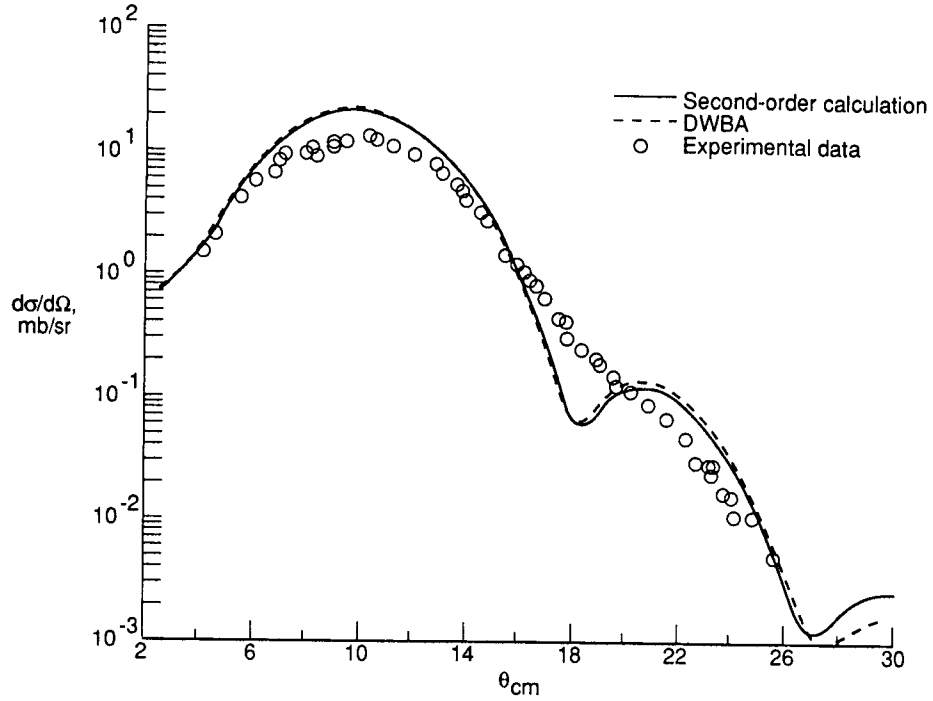

Figure 10. Theoretical and experimental (ref. 20) inelastic angular distributions for excitation of 3^- state in ^{12}C in 1040 MeV p–^{12}C scattering.

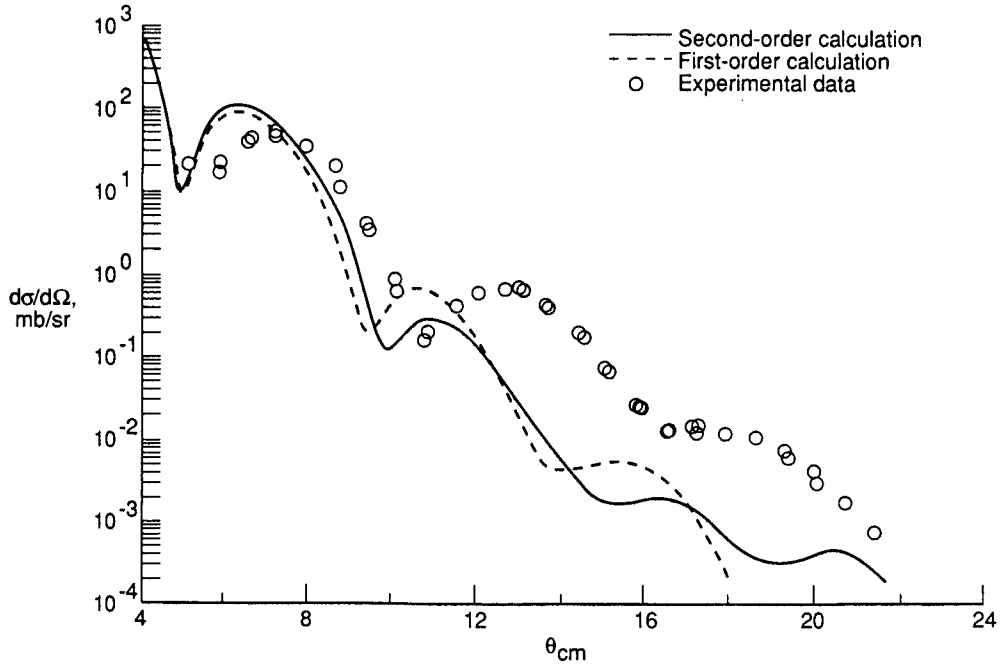

Figure 11. Theoretical and experimental (ref. 21) elastic angular distributions for 340A MeV α–^{12}C scattering.

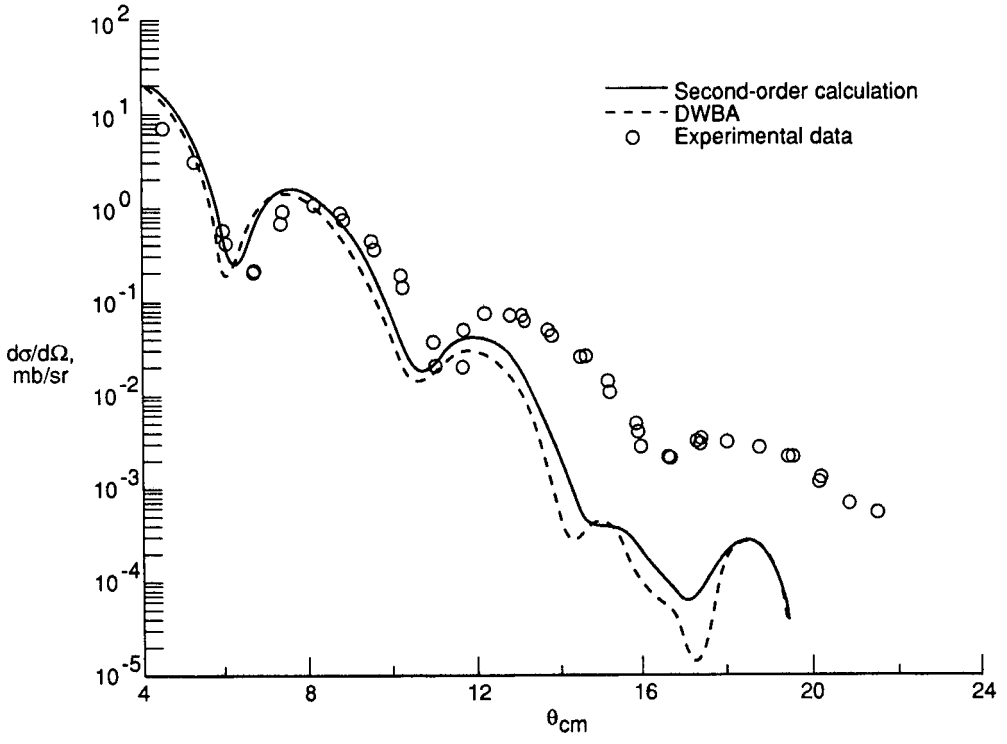

Figure 12. Theoretical and experimental (ref. 20) inelastic angular distributions for excitation of 0^+ state in ^{12}C in 340A MeV α–^{12}C scattering.

NASA
National Aeronautics and Space Administration

Report Documentation Page

1. Report No.	2. Government Accession No.	3. Recipient's Catalog No.
NASA TP-2830		

4. Title and Subtitle	5. Report Date
Eikonal Solutions to Optical Model Coupled-Channel Equations	November 1988
	6. Performing Organization Code

7. Author(s)	8. Performing Organization Report No.
Francis A. Cucinotta, Govind S. Khandelwal, Khin M. Maung, Lawrence W. Townsend, and John W. Wilson	L-16462
	10. Work Unit No. 199-22-76-01

9. Performing Organization Name and Address	11. Contract or Grant No.
NASA Langley Research Center Hampton, VA 23665-5225	

12. Sponsoring Agency Name and Address	13. Type of Report and Period Covered
National Aeronautics and Space Administration Washington, DC 20546-0001	Technical Paper
	14. Sponsoring Agency Code

15. Supplementary Notes

Francis A. Cucinotta, Govind S. Khandelwal, and Khin M. Maung: Old Dominion University, Norfolk, Virginia.

Lawrence W. Townsend and John W. Wilson: Langley Research Center, Hampton, Virginia.

16. Abstract

Methods of solution are presented for the eikonal form of the nucleus-nucleus coupled-channel scattering amplitudes. Analytic solutions are obtained for the second-order optical potential for elastic scattering. A numerical comparison is made between the first- and second-order optical model solutions for elastic and inelastic scattering of ^{1}H and ^{4}He on ^{12}C. The effects of bound-state excitations on total and reaction cross sections are also estimated.

17. Key Words (Suggested by Authors(s))	18. Distribution Statement
Heavy ion collisions Eikonal approximation Coupled channels	Unclassified—Unlimited Subject Category 73

19. Security Classif.(of this report)	20. Security Classif.(of this page)	21. No. of Pages	22. Price
Unclassified	Unclassified	28	A03

For sale by the National Technical Information Service, Springfield, Virginia 22161-2171